Biomaterials 159 (2018) 174–188

Contents lists available at ScienceDirect

Biomaterials

journal homepage: www.elsevier.com/locate/biomaterials

Efficient and cost-effective generation of hepatocyte-like cells through microparticle-mediated delivery of growth factors in a 3D culture of human pluripotent stem cells

Zeinab Heidariyan [a], Mohammad Hossein Ghanian [b], Mohsen Ashjari [c], Zahra Farzaneh [a], Mostafa Najarasl [a], Mehran Rezaei Larijani [a], Abbas Piryaei [d, e], Massoud Vosough [a], Hossein Baharvand [a, f, *]

[a] Department of Stem Cells and Developmental Biology, Cell Science Research Center, Royan Institute for Stem Cell Biology and Technology, ACECR, Tehran, Iran
[b] Department of Cell Engineering, Cell Science Research Center, Royan Institute for Stem Cell Biology and Technology, ACECR, Tehran, Iran
[c] Chemical Engineering Department, Faculty of Engineering, University of Kashan, Kashan, Iran
[d] Department of Biology and Anatomical Sciences, School of Medicine, Shahid Beheshti University of Medical Sciences, Tehran, Iran
[e] Department of Tissue Engineering and Applied Cell Sciences, School of Advanced Technology in Medicine, Shahid Beheshti University of Medical Sciences, Tehran, Iran
[f] Department of Developmental Biology, University of Science and Culture, Tehran, Iran

ARTICLE INFO

Article history:
Received 9 August 2017
Received in revised form
31 December 2017
Accepted 1 January 2018
Available online 2 January 2018

Keywords:
Growth factor delivery
Microparticles
Hepatocyte-like cells
Human pluripotent stem cells
Hepatic organoid

ABSTRACT

Biomedical application of human pluripotent stem cell-derived hepatocyte-like cells (hPSC-HLCs) relies on efficient large-scale differentiation, which is commonly performed by a suspension culture of three-dimensional (3D) multicellular spheroids in bioreactors. However, this approach requires large amounts of growth factors (GFs) and the need to overcome limited diffusional transport posed by the inherent 3D structure of hPSC spheroids. Here, we have hypothesized that localized delivery of GFs by incorporation of GF-laden degradable polymeric microparticles (MPs) within the hPSC spheroids would circumvent such limitations. In this study, GFs for hepatocytic differentiation were encapsulated in gelatin-coated poly (L-lactic acid)/poly (DL-lactic-co-glycolic acid) (PLLA/PLGA) MPs which were subsequently incorporated into the hPSC spheroids. Gene expression analyses demonstrated that MP delivery of the GFs resulted in similar expression levels of hepatocytic markers despite the use of 10-fold less total GFs. The differentiated HLCs in the MP group exhibited ultrastructure and functional characteristics comparable with the conventional soluble GF group. The generated HLCs in the MP group were successfully engrafted in an acute liver injury mouse model and maintained hepatocytic function after implantation. These results suggested that sustained and localized delivery of GFs using MPs might offer a novel approach towards scalable technologies for hepatocytic differentiation and engineer a better 3D microenvironment for cells.

1. Introduction

Human pluripotent stem cell-derived hepatocyte-like cells (hPSC-HLCs) provide a potential supply for hepatic tissue engineering, drug screening, and cell-based therapies [1]. Thus, a scalable, efficient and cost-effective protocol that differentiates hPSCs into hepatocytes in a bioreactor is a crucial step toward their biomedical applications. In recent years, three-dimensional (3D) cell cultures (spheroids) have been used for expansion of hPSCs [2] and hepatocytic differentiation of hPSCs [3,4], successful engraftment of the transplanted hPSC-HLCs [5], and maintenance of hepatocytes [6,7]. Spheroid cultures in suspension provide a 3D environment with efficient cell-cell contacts [8]. However, there are two pivotal challenges for scalable hepatocytic differentiation of hPSCs. First, consecutive renewal of soluble growth factors (GFs) is necessary in the conventional approach in 3D differentiation of hPSCs. This is costly because of the high consumption of GFs.

* Corresponding author. Royan Institute, Banihashem Sq., Banihashem St., Resalat Highway, P.O. Box 16635-148, Tehran 1665659911, Iran.
E-mail address: baharvand@royaninstitute.org (H. Baharvand).

https://doi.org/10.1016/j.biomaterials.2018.01.005
0142-9612/

Second, these 3D spheroids have size limitations due to insufficient diffusion of soluble GFs into the spheroids [9,10]. The outer layer of spheroids is exposed to higher concentrations of soluble GFs, whereas cells in the core part receive lower amounts. According to Fick's law of diffusion, inner regions are exposed to lower levels of GFs because this requires more time to reach the central regions of the spheroids [10]. Furthermore, the dense shell on the surface and marginal zone that contains collagen I, tight cell–cell junctions, and a basement membrane have been shown to hinder diffusion based transport from the outside [9,11]. The microenvironment within cell spheroids varies by location because of cell–cell interactions, diffusional constraints, and secretion of matrix and paracrine factors [11].

One approach to overcome these problems in 3D differentiation of hPSCs could be the incorporation of microparticles (MPs) within the hPSC spheroids for sustained release and homogenous distribution of morphogens throughout the spheroids (for review see Refs. [12,13]). Morphogen-loaded biodegradable MPs are widely used as inside-out delivery vehicles in differentiation of multicellular spheroids of mesenchymal stem cells, neural stem cells, and embryonic stem cells (ESCs) into germ cells [14], mesoderm and ectoderm lineage derivatives [15], primitive streak cells [16], blood cells [17], osteogenic or angiogenic cells [18,19], chondrocytes [20], tendon cells [21] and mature neurons [22]. The ability to localize morphogens within spheroids by MP-mediated delivery has been used for spatiotemporal control of differentiation within 3D cultures. However, to the best of our knowledge, there is no report about the application of GF controlled release by MPs for efficient directed differentiation of hPSCs to hepatocytes in a suspension culture.

We have hypothesized that the incorporation of GF-laden degradable polymeric MPs within human embryonic stem cell (hESC) spheroids would circumvent such limitations in the 3D suspension culture and result in efficient hepatocytic differentiation. To address this hypothesis, we first documented the characteristics of poly (L-lactic acid)/poly (DL-lactic-co-glycolic acid) (PLGA/PLLA) MPs loaded with two key GFs for hepatocytic differentiation [hepatocyte growth factor (HGF) and fibroblast growth factor 4 (FGF4)]. Then, we aggregated hESCs with GF-loaded MPs within the 3D culture suspension and differentiated them into a hepatocytic fate. We reduced the total consumption of GFs to one-tenth by MP delivery to have a cost-efficient application of GFs in large-scale differentiation in a bioreactor. Compared to the conventional soluble delivery method, gene expression analyses demonstrated that incorporation of GF-loaded MPs resulted in similar expression levels of hepatocytic markers, ultrastructure, and functional characteristics. These results suggested that MP delivery of GFs with less consumption might offer a novel approach towards overcoming the current limitations associated with scalable suspension technologies of 3D hPSC spheroids and engineer a more efficient 3D microenvironment for biomedical applications of hPSCs.

2. Materials and methods

2.1. Fabrication of microparticles (MPs)

We used PLGA (50:50, Resomer® RG 504 H, Sigma-Aldrich) to fabricate the microspheres according to the water-in-oil-in-water double emulsion solvent extraction technique. We prepared two separate solutions of 40 mg PLLA/PLGA (1:1) in 2.5 ml dichloromethane (DCM), and 4.5 μg each of HGF and FGF4 in 0.6 ml phosphate-buffered saline (PBS) supplemented with GF stabilizers [heparin and bovine serum albumin (BSA, Sigma-Aldrich, A3311)]. Next, the polymer organic solution and GF aqueous solution were mixed and emulsified by homogenization at 6000 rpm for 2 min. The prepared single emulsion was immediately emulsified in 200 ml of dH_2O that contained 0.1% w/v methylcellulose and 1% w/v PVA by a mechanical stirrer at 400 rpm to produce a water-in-oil-in-water double emulsion. The methylcellulose solution used in this emulsification step was partially saturated by the addition of 1.8 ml DCM to prolong the extraction of DCM from the oil droplets by water and prevent premature hardening of the microspheres before the two polymers could phase separate. Controlled extraction of DCM and hardening of the polymer droplets were initiated after 30 min by the addition of another 200 mL of a 0.1% w/v methylcellulose solution without DCM. This extraction was performed with a peristaltic pump at a rate of 1 mL/min and stirring at room temperature (RT). The resultant hardened microspheres were filtered, washed with water, and freeze-dried overnight. Blank MPs were produced similarly, except we did not use GF in the first water phase. A total of 10 μg of CellTracker Red (CTR; Biotechnology; C34552) was dissolved into DCM prior to preparation of the emulsion to produce fluorescent-labeled MPs to track the MPs in spheroids. The prepared MPs were morphologically analyzed by scanning electron microscopy (SEM, VEGA\TESCAN) and the particle size distribution was determined by dynamic light scattering (DLS, Mastersizer 2000, Malvern).

2.2. Growth factor (GF) release from microparticles (MPs)

We investigated GF release profiles from the MPs by suspending 5 mg of gelatin-coated MPs into 0.5 mL of PBS supplemented with 0.02% Tween 20 and 10 mg/ml BSA. The MPs were incubated at 37 °C. The samples were centrifuged and the entire supernatant collected at specific time points over a period of 20 days. Next, we added fresh release medium. The supernatants were stored at −20 °C until the HGF and FGF4 contents were quantified by enzyme-linked immunosorbent kits (ELISA; R&D Systems). Concentrations of GFs were determined by comparison to standard curves. All analyses were conducted in duplicate.

To determine encapsulation efficiency, 5 mg of the GF-loaded microspheres was dissolved in 1 ml NaOH (1 N), which contained 1% SDS by stirring for 24 h at RT. Then, the clear solution was centrifuged for 5 min at 5000 rpm. The supernatant was analyzed by a BCA kit (Pierce BCA Protein Assay Kit; Thermo Fisher Scientific) to measure the total protein content. The loading efficiency was calculated using (m2/m1x100) where m2 was the measured weight of protein in MPs and m1 was the total weight of protein used for MP fabrication.

2.3. Three-dimensional (3D) cell spheroid formation

We used the RH5 hESC line [23]. A total of 3×10^5 live cells/mL were transferred to low attachment bacterial plates (60 mm; Griner, 628102) with 5 mL of hESC medium and conditioned for 24 h on inactivated human foreskin fibroblasts (HFFs) with mitomycin C (Sigma-Aldrich; M0503) [2,24]. hESC medium included Dulbecco's modified Eagle's medium (DMEM/F12; Gibco, 21331–020), 20% knockout serum replacement (KOSR; Gibco, 10828–028), 0.1 mM β-mercaptoethanol (Sigma-Aldrich; M7522), 1% penicillin and streptomycin (Gibco; 15070–063), 1 mM nonessential amino acids (Gibco; 11140–035), 2 mM L-glutamine (Gibco; 25030–024), 1% insulin–transferrin–selenium (ITS; Gibco, 41400–045), and 100 ng/mL bFGF (Royan Biotech).

For MP incorporation, the UV-sterilized PLGA MPs were coated with gelatin *via* a sonication-mediated suspension in a sterile gelatin solution (0.1% w/v) and incubated for 3 h at RT with mild stirring, followed by centrifugation. We subsequently removed the supernatant and washed the MPs twice with PBS. The gelatin-

coated MPs were re-suspended in culture medium. We used a hemocytometer to determine particle density. Finally, we mixed the desired volumes of the MP and hESC suspensions to obtain a cell to MP ratio of 3:1. The plates were incubated under standard conditions (37 °C, 5% CO_2, and saturated humidity). After 24 h, the single cells successfully aggregated.

2.4. Hepatocytic differentiation procedure

After spheroid formation, we changed the media of the plates to differentiation medium. Fig. 2A shows the stepwise differentiation protocol of hESCs to HLCs. There were three stages: definitive endoderm formation (DE, 3 days), hepatoblast (HB, 7 days), and hepatocyte-like cell (HLC, 10 days). During DE formation the medium consisted of RPMI 1640 (Invitrogen; 51800), 0.1% BSA, and 1% B27 (Gibco; 12587–010). The medium was supplemented with 6 μM CHIR99021 (Stemgent; 04-0004-10) for one day followed by 10 ng/ml activin A (R&D Systems; 338-AC) for two days. In the HB stage, the base medium DMEM-F12 was supplemented with 2% KOSR, 10 ng/ml HGF (R&D Systems, 294-HG), and 10 ng/ml FGF4 (Royan Biotech) for 7 days. Then, the cells were treated for an additional 10 days in a 1:1 ratio of hepatocyte basal medium (HBM; Lonza, CC-3199) and DMEM/F12 that contained 2% KOSR, 10 ng/mL oncostatin M (OSM; R&D Systems, 295-OM), 0.1 mM dexamethasone (Dex; Sigma-Aldrich, D-2915), 1 mM nonessential amino acids, and L-glutamine. The hepatocytic differentiation protocols were the same for both soluble GF delivery [S (1X)] and MP-mediated GF delivery [MP (0.1X)] groups, except that the later received HGF and FGF4 *via* MP-delivery instead of the soluble form.

2.5. Gene expression assay

We used quantitative real-time reverse transcriptase polymerase chain reaction (qRT-PCR) to verify the cell expression profile during differentiation. Total RNA was extracted with TRIzol (Sigma-Aldrich, T9424), then treated with an RNase-free DNase (Takara, 2270A1) to eliminate cDNA. Next, cDNA was generated with a RevertAid First Strand cDNA Synthesis Kit (Takara kit) based on the manufacturer's instructions. Duplicate qRT-PCR reactions were performed with the SYBR Green Master Mix (Takara Bio, Inc., SYBR Premix Ex Taq II RR081Q) by the real-time PCR system (Corbett Life Science; Rotor-Gene 6000 instrument) and analyzed with Rotor-Gene 6000 analysis software (Corbett Life Science; version 1.7). The samples were collected from three independent biological replicates. The expression levels of the desired genes were normalized to glyceraldehyde 3-phosphate dehydrogenase (*GAPDH*) as the reference gene and then normalized to corresponding stem cells. The expression profile of differentiated cells in different groups was compared to a hepatocytic cell line, Huh7 as the positive control. Analysis was performed by the comparative CT method ($2^{-\Delta\Delta Ct}$). Primers are listed in Supplementary Table S1.

2.6. Immunofluorescence assay

Spheroids of HLCs were collected at the end of day 20. The spheroids were washed with PBS and fixed overnight at 4 °C with 4% (w/v) paraformaldehyde (Sigma-Aldrich, P6148). Then, spheroids were embedded in agar gel and subsequently embedded in paraffin blocks. The 6 μm sections were prepared and deparaffinized. Next, sections were treated with antigen retrieval (Dako) and then permeabilized by using 0.1% Triton X-100 for 10 min. For blocking, we used 10% goat serum (SAFC Bioscience, 12306 C) in PBS for 1 h at 37 °C. The slides were incubated overnight with primary antibodies at 4 °C. Finally, the sections were washed 4 times and incubated with secondary antibodies for 1 h at 37 °C. Nuclei were counter-stained with 0.5 μg/ml of 4′,6-diamidino-2-phenylindole (DAPI, Sigma-Aldrich, D8417) for 1 min. The immunofluorescent micrographs were taken with a fluorescent microscope (BX51; Olympus, CP70 camera). For the negative control, we applied the same staining procedure without primary antibodies. Supplementary Table S2 summarizes the list of antibodies.

2.7. Flow cytometry analysis

Differentiated cells in hepatocytic-like spheroids were dissociated by trypsin, fixed in 4% paraformaldehyde for 20 min at RT, permeabilized in 0.1% Triton X-100 for 10 min at RT, and blocked in 10% secondary antibody host serum in 0.5% BSA for 1 h at RT. Next, HLCs were incubated overnight with primary antibodies at 4 °C. Primary and secondary antibodies were the same as those used for immunofluorescence staining. Flow analysis was performed using a BD-FACS Calibur flow cytometer (FACSCalibur). Analyses were performed on three independent biological experiments. Data were analyzed using the Flowing software (version 2.5.1, Turku Centre for Biotechnology).

2.8. Cytochrome P (CYP) activity and inducibility

We have used the ethoxyresorufin-O-deethylase (EROD) and pentoxyresorufin O-dealkylase (PROD) assays to evaluate CYP450 enzyme activity. Ethoxyresorufin and pentoxyresorufin are nonfluorescent substrates which are O-deethylated and O-dealkylated by the CYP450 system (CYP2B1/2 and CYP1A1, respectively) and converted into resorufin, a red fluorescent substance. Hepatocytic-like spheroids were incubated with 2 mM phenobarbital (PB) for 3 days. Next, the spheroids were washed and transferred into medium that contained 5 mM 7-ethoxyresorufin (Sigma-Aldrich; E3763) or 7-pentoxyresorufin (Sigma-Aldrich; P9049) and 80 mM dicumarol (Sigma-Aldrich; M1390) in Hank's balanced salt solution. The plates were incubated at 37 °C for 30 min. The supernatant from the spheroids was collected for a fluorescent intensity assay using a BioTek plate reader (BioTek Synergy™ 4).

2.9. Indocyanine green (ICG) uptake assay

Differentiated hepatocytic-like spheroids were incubated with indocyanine green (ICG, 1 mg/ml; Sigma-Aldrich, 12633) for 1 h at 37 °C according to the manufacturer's instructions. Uptake of ICG was visualized with a light microscope.

2.10. Low-density lipoprotein (LDL) uptake assay

Low-density lipoprotein (LDL) uptake assay was performed using Dil-Ac-LDL (Biomedical Technologies, Inc., BT-902) according to the manufacturer's instructions. Fluorescent images were captured by a fluorescent microscope (IX71, Olympus).

2.11. Periodic acid-Schiff (PAS) staining

We evaluated the capacity of differentiated hepatocytic-like spheroids to store glycogen. Hepatocytic-like spheroids at day 20 were evaluated by the periodic acid-Schiff (PAS) method. Briefly, the spheroid sections were oxidized in 1% periodic acid for 5 min and rinsed in dH_2O. Sections were subsequently treated with Schiff's reagent for 15 min following color development in dH_2O for 5–10 min.

2.12. Albumin (ALB) and urea production assays

After 48 h incubation, conditioned media from differentiated hepatocytic-like spheroids were collected and stored at −20 °C. The amount of ALB secreted into the culture media was quantified using a human ALB ELISA kit (Bethyl, E80-129) according to the manufacturer's instructions with a microplate reader (Thermo Scientific, Multiskan Spectrum, 51118650). The amount of urea produced was determined by a colorimetric assay kit (Biorexfars, BXC0126A, 941210) according to the manufacturer's instructions. The results were normalized to total protein (Total Protein Kit, Biorex, BXC0173A, 921239) according to the manufacturer's instructions. All tests were carried out in three biological replicates. The data from ALB secretion and urea production of primary human hepatocytes were used as positive controls in this study.

2.13. Transmission electron microscopy (TEM)

We observed the ultrastructure of the hepatocytic-like spheroids by transmission electron microscopy (TEM). Spheroids were washed twice with PBS, pre-fixed with 2.5% glutaraldehyde in 0.1 M PBS (pH 7.4) for 2 h, and then post-fixed with 1% osmium tetroxide for 1.5 h. The spheroids were dehydrated in a graded acetone series and embedded in epoxy resin (TAAB, UK). Then, 60–70 nm (silver-grade) sections were prepared by an ultra-microtome (Leica Ultra Cut UC6, Austria). The sections were double-stained with 5% uranyl acetate and 0.5% lead citrate, then visualized using a Zeiss EM 900 transmission electron microscope (Germany) with an accelerating voltage of 50 kV.

2.14. Cell transplantation in an animal model

Acute liver injury was induced in 10-week old male NMRI mice by an intraperitoneal injection of 0.6 ml/kg of CCl4 (Sigma-Aldrich). We used four animal groups for the *in vivo* experiment: healthy mice (normal), acute liver injury model (control), and acute liver injury model with transplanted HLCs differentiated by S (1X) or MP (0.1X) treatments. Hepatocytic-like spheroids were enzymatically dissociated into single cells and labeled with PKH26 (Red Fluorescent Cell Linker Kit, Sigma-Aldrich; P9691) according to the manufacturer's instructions. The S (1X) and MP (0.1X) transplanted groups received intrasplenic injections of 1×10^6 cells 24 h after induction of acute liver injury. The transplanted animals were immunosuppressed with daily cyclosporine (Novartis Pharmaceuticals, 20 mg/kg) 4 days before cell transplantation until one week after transplantation. The normal group in this study received immunosuppression, whereas the control group received immunosuppression and CCl4 injection. After one week, the blood samples were collected and the levels of alanine transaminase (ALT), aspartate transaminase (AST), alkaline phosphatase (ALP), and total bilirubin were measured by commercially available kits (Biorexfars, BXC0215A, BXC0205A, BXC0185A, BXC0191A). Human ALB (hALB) was quantified by the hALB ELISA Kit (Bethyl; E80-129). Liver samples were collected for histologic analysis to track the engrafted cells. The liver samples were fixed in 10% formalin and enblocked in paraffin. Then, the nuclei in the liver tissues of the 6 μm sections were counterstained with DAPI (Sigma; D8417). The slides were visualized by a fluorescent microscope (BX51; Olympus). We assessed the number of PKH-positive cells compared to the total number of cells in at least 30 stochastically selected fields for each group to quantify the number of engrafted cells. An immunofluorescent assay was performed to evaluate the expression of hALB in PKH-positive cells. All procedures and samples used in this study received approval from the Royan Institutional Review Board and Institutional Ethical Committee of Royan Institute (No: EC/93/1031).

2.15. Statistical analysis

Data are presented as mean ± standard deviation (SD) from at least three biological replicates. Comparisons were made with the student's t-test or one way-analysis of variance (ANOVA), followed by Tukey's post-test. P-values less than 0.05 were considered significant.

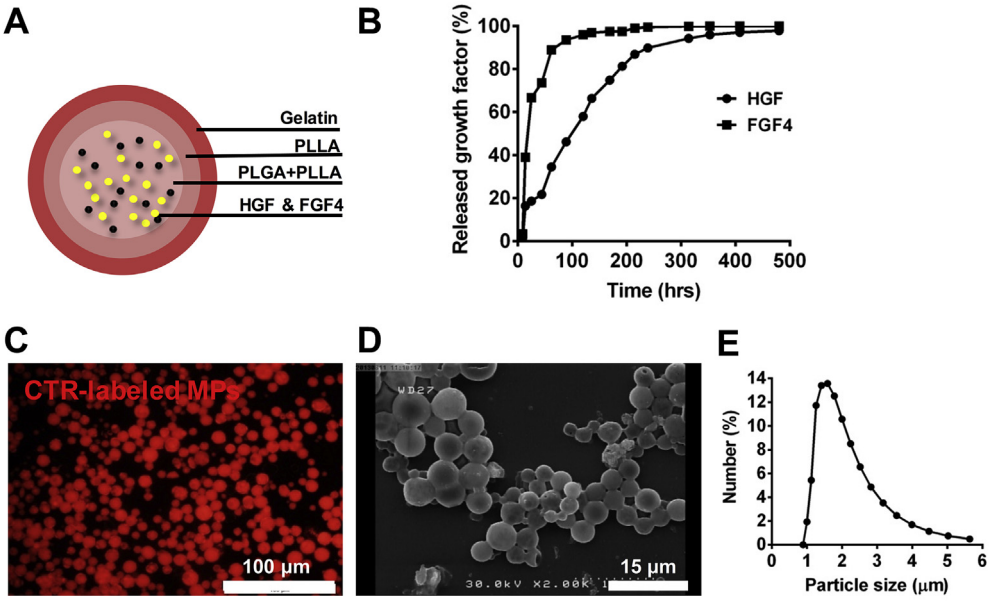

Fig. 1. Preparation and characterization of microparticles (MPs). (A) Schematic representation of growth factor (GF)-loaded poly (L-lactic acid)/poly (DL-lactic-co-glycolic acid) (PLGA/PLLA) microparticles (MPs) produced by the modified double emulsion method. (B) Release profile of hepatocyte growth factor (HGF) and fibroblast growth factor 4 (FGF4) from MPs over a 20-day period. (C) CellTracker Red (CTR)-labeled MPs. (D) Representative scanning electron microscopy (SEM) of MPs. (E) Size distribution histogram of MPs: 2.01 ± 0.97 μm. (For interpretation of the references to color in this figure legend, the reader is referred to the Web version of this article.)

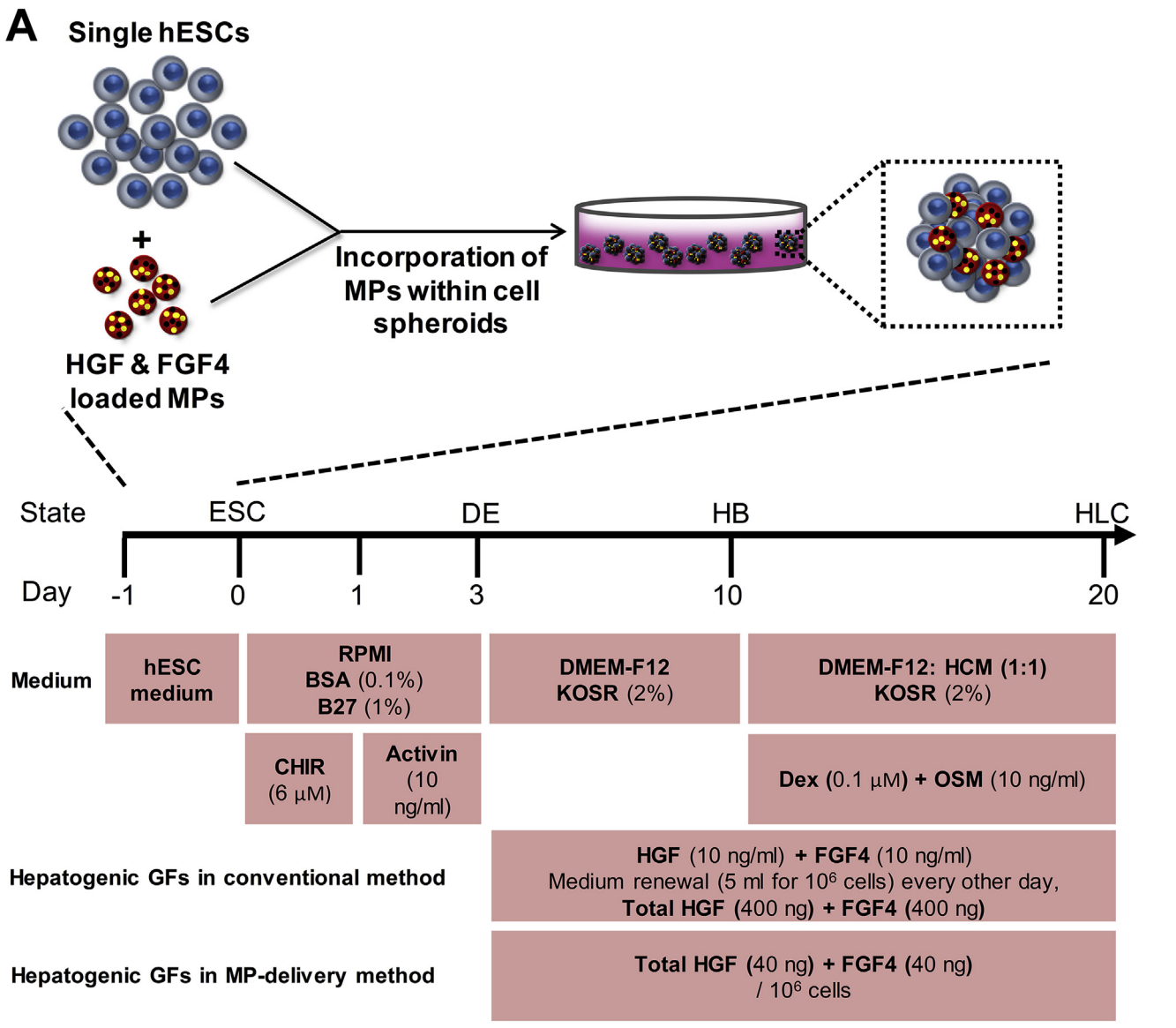

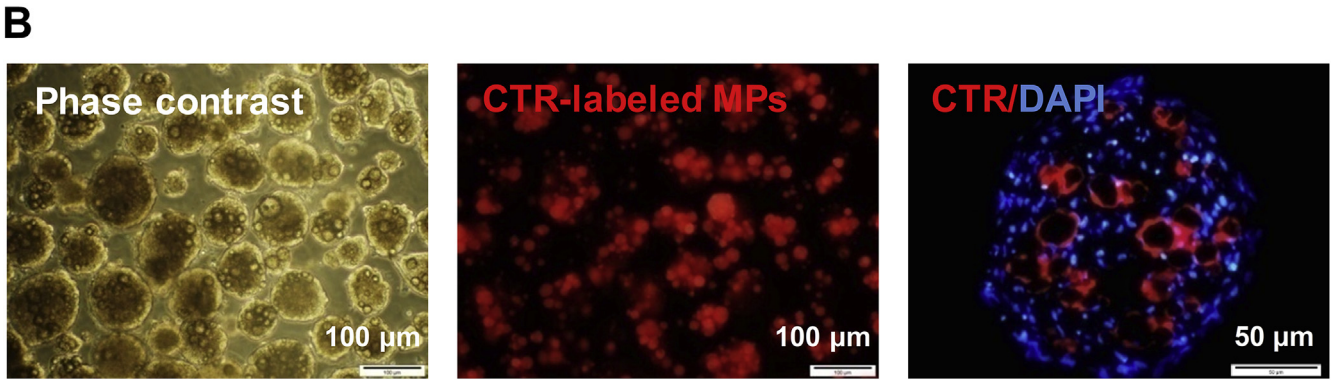

Fig. 2. Incorporation of MPs within human embryonic stem cell (hESC) spheroids to produce hepatocyte-like cells (HLCs). (A) Schematic representation of stepwise protocol for differentiation of hESCs towards HLCs. CTR-labeled MPs were mixed with single hESCs (3:1 cell to MP ratio) and MP-incorporated spheroids formed after 24 h. The differentiation protocol of hESCs to HLCs included three steps: definitive endoderm formation (DE, 3 days), hepatoblast generation (HB, 7 days), and HLC maturation (10 days). The hepatocytic differentiation protocol was the same for both the S (1X) and MP (0.1X) groups, except that the latter received hepatocyte growth factor (HGF) and fibroblast growth factor 4 (FGF4) *via* MP-delivery instead of the soluble form. Total GF consumption was 400 ng for each HGF and FGF4 per replicate in the conventional soluble method (10 ng/ml x 8 times medium renewal x 5 ml medium per renewal), whereas it was 40 ng for each GF in the MP delivery method. We used 5 ml medium per plate. Based on the measured GF of 56 ng GF/mg MP and the particle density of 5×10^5 particles/mg MP, a one-tenth consumption of GFs was obtained by using a 3:1 cell to MP ratio. (B) GF-loaded MPs were incorporated successfully within the stem cell spheroids. Phase contrast microscopy image (left), fluorescence microscopy image (middle), and paraffin-embedded cross section (right) of CTR-labeled MPs in 24 h incorporated hESC spheroids. CTR-labeled MPs are visualized in red. The nuclei of cells counterstained with DAPI. (For interpretation of the references to color in this figure legend, the reader is referred to the Web version of this article.)

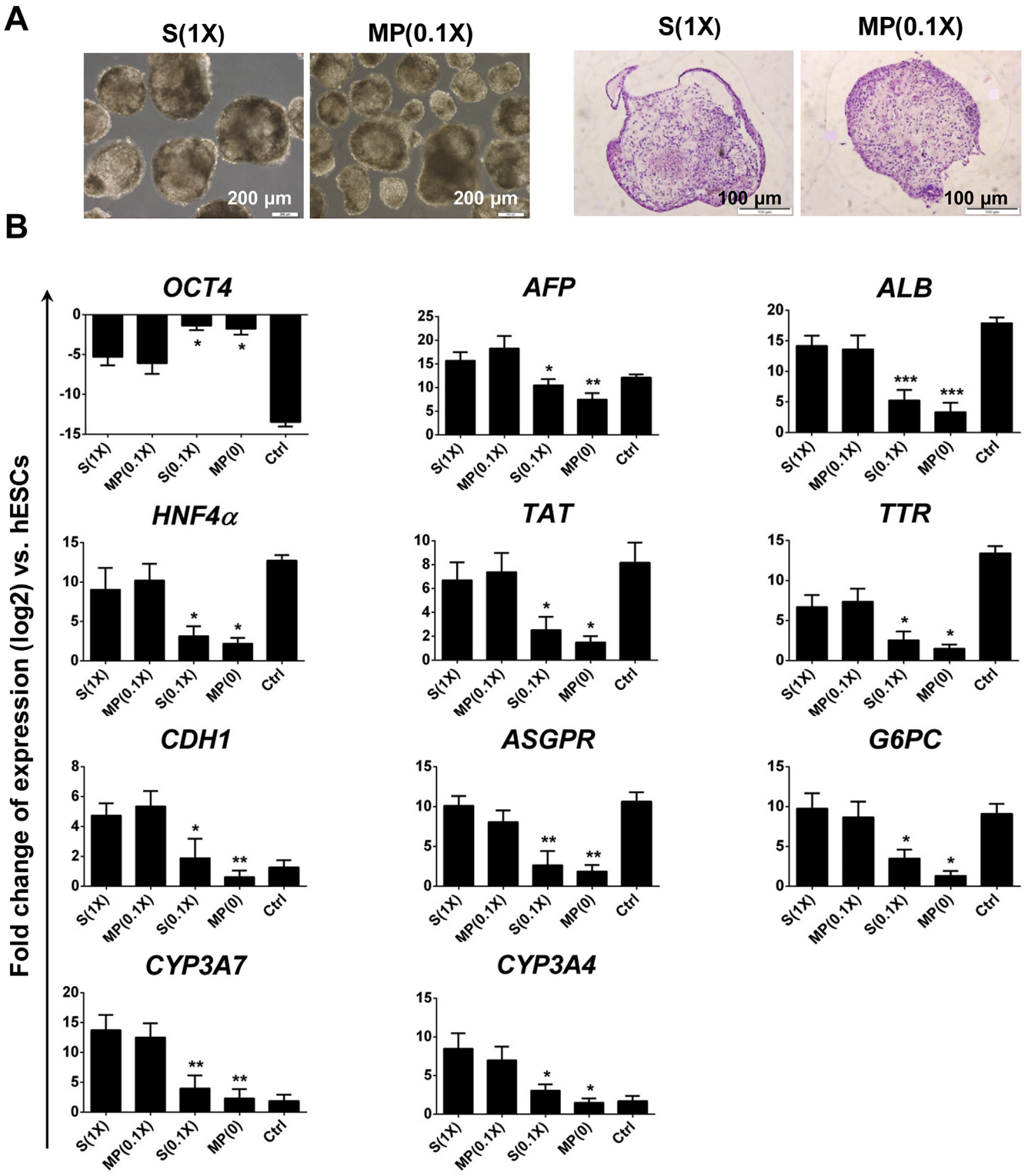

Fig. 3. Morphology and gene expression of hESC-HLCs. (A) Phase contrast microscopy image (left) and H&E stained sections (right) of HLC spheroids differentiated from hESCs at day 20 of differentiation. No significant differences in the morphology of spheroids existed between soluble (S) and MP-mediated delivery methods. (B) HGF and FGF4 delivered from MPs or added to the medium induced hepatocytic gene expressions. Directed differentiation by MP delivery of HGF and FGF4 in the MP (0.1X) group induced comparable levels of hepatocytic-specific gene expression compared to soluble delivery of the same GF in the S (1X) group. There were no significant differences in hepatocytic-specific gene expressions between the soluble or MP-mediated delivery groups. A hepatocytic cell line (Huh7) was used as the positive control (Ctrl). Data were normalized to *GAPDH* and represented as fold change compared with hESCs, set to 1 as the calibrator. *: $P < .05$, **$P < .01$ (one-way ANOVA with Tukey's post hoc) between S (1X) and MP (0.1X) groups. Data are shown as mean ± SD ($n = 3$). Culture medium: MP (0).

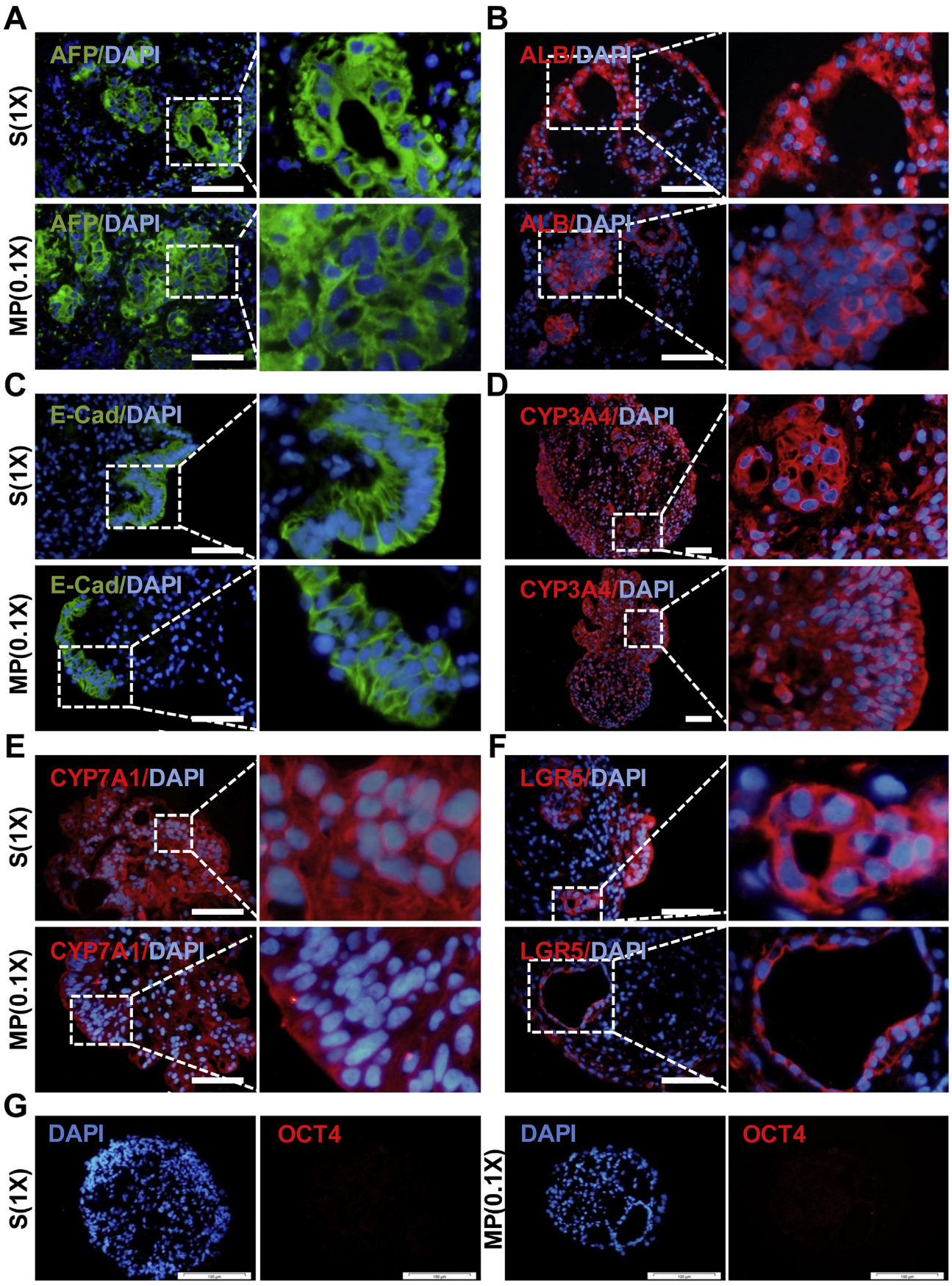

Fig. 4. Protein expression of hESC-HLCs. Immunofluorescence staining of (A) α-fetoprotein (AFP), (B) albumin (ALB), (C) E-cadherin, (D) CYP3A4, (E) CYP7A1, (F) LGR5, and (G) OCT4 on day 20 of differentiation. The nuclei were counterstained with DAPI. Scale bar: 50 μm.

3. Results

3.1. Production and characterization of microparticles (MPs)

PLGA is a biocompatible and biodegradable polymer commonly used for MP-mediated delivery of GFs. Biodegradability of PLGA is governed by hydrolyzation into lactic acid and glycolic acid which are natural by-product metabolites [25]. Although GF release from PLGA microspheres can be controlled by creating variations in the polymer properties of molecular weight, copolymer ratio and crystallinity, it usually suffers from an initial burst release [25,26]. In this study, we have used a modified double emulsion method to produce PLGA/PLLA MPs with minimal burst release (Fig. 1A). MP incorporation within the spheroids was the first validated challenge step prior to the differentiation steps. Cell-MP interaction is necessary for efficient incorporation [27]. Therefore, we coated the surface of MPs with a thin layer of gelatin before mixing them with single hESCs (Fig. 1A). Analysis of protein loading showed that approximately 50% of the GFs loaded within the MPs. Fig. 1B shows the release profiles of HGF and FGF4 from MPs over 20 days. MPs were labeled with CTR for tracking after incorporation within the cell spheroids (Fig. 1C). According to DLS analysis, the MPs had a mean diameter of 2.01 ± 0.97 μm (Fig. 1D and E).

Initially we examined various cell to MP ratios. We observed an efficient spheroid formation at a 3:1 cell to MP ratio in hESC medium. After 24 h, the MPs successfully incorporated within the cell spheroids (Fig. 2A). This ratio was selected to avoid the effects of differentiation by the MPs [15]. Immunofluorescent microscopy showed homogenous distribution of the CTR-labeled MPs throughout the hESC spheroids (Fig. 2B). Repeatedly, by using approximately 2 mg of lyophilized MPs, we measured the particle number as 10^6 particles, which was considered the base for calculating the required amount of MPs. Fig. 2A shows the stepwise differentiation protocol of hESCs to HLCs that included three steps: DE (3 days), HB (7 days) and HLC maturation (HLC, 10 days). The hepatocytic differentiation protocol was the same for both the S (1X) and MP (0.1X) groups, except that the latter received HGF and FGF4 *via* MP-delivery instead of the soluble form. Total GF consumption was 400 ng/10^6 cells for each HGF and FGF4 (Fig. 2A). Based on the measured GF content of 56 ng GF/mg MP and particle density of 5×10^5 particles/mg MP, we obtained a one-tenth consumption of GFs by using the 3:1 cell to MP ratio.

3.2. Characterization of hepatocyte-like cell (HLC) differentiation via microparticle (MP) delivery of growth factors (GFs) in spheroids

3.2.1. Morphological and gene expression analyses

After 20 days of differentiation, we observed no significant differences between the S (1X) and MP (0.1X) groups in cell spheroid morphology as demonstrated by phase contrast microscopy and hematoxylin and eosin (H&E) stained cross-sections (Fig. 3A). Both groups contained cystic and dense spheroids. However, the majority were dense spheroids (75%). We also analyzed mRNA expressions of the pluripotency marker, *OCT4,* and hepatocyte-specific genes α-fetoprotein (*AFP*), *ALB*, hepatocyte nuclear factor 4α (*HNF4α*), tyrosine aminotransferase (*TAT*), transthyretin (*TTR*), E-cadherin (*CDH1*), asialoglycoprotein receptor (*ASGPR*), glucose-6-phosphatase (*G6PC*), and cytochrome P450 subunits 3A7 (*CYP3A7*) and 3A4 (*CYP3A4*) by qRT-PCR (Fig. 3B). We observed significant downregulation of *OCT4* during differentiation in the presence of GF in both the S and MP groups (Fig. 3B). MP-mediated delivery of HGF and FGF4 resulted in similar upregulation of the hepatocytic specific genes with no significant differences with the soluble group (Fig. 3B). The use of 10-fold less GFs in conventional soluble delivery without MPs [S (0.1X)] significantly decreased expressions of the hepatocytic genes compared to S (1X) and MP (0.1X) groups (at least $P < .05$, Fig. 3B). The presence of unloaded MPs within the cell spheroids without HGF and FGF4 in the culture medium [MP (0)] significantly decreased expressions of the hepatocytic genes compared to the S (1X) and MP (0.1X) groups (at least $P < .05$, Fig. 3B). These results suggested that, compared to treatment with S (1X), MP (0.1X) delivery of HGF and FGF4 within hESC spheroids resulted in similar expressions of hepatocyte-specific genes.

Immunofluorescence staining on day 20 showed that the cells in both the S (1X) and MP (0.1X) groups expressed hepatocytic markers, AFP (Fig. 4A), ALB (Fig. 4B), E-cadherin (Fig. 4C), CYP3A4 (Fig. 4D), CYP7A1 (Fig. 4E), and LGR5 (Fig. 4F). However, the pluripotency marker OCT4 was not detectable in HLCs in both groups (Fig. 4G).

In addition, flow cytometry analysis was performed on day 20. Spheroids treated in S (1X) and MP (0.1X) groups showed no significant difference for expressions of AFP and ALB. Approximately 50% of cells expressed these markers in both groups (Fig. 5).

Ultrastructural analysis of differentiated cells demonstrated a considerable difference in the S (1X) and MP (0.1X) groups when compared with hPSCs [28]. We observed some similarities to immature hepatocytes (Fig. 6) [29,30]. TEM analysis showed microvilli (MV) at the apical side of the differentiated cells with abundant cell–cell contacts that consisted of tight junctions (TJ). There were other intercellular junctions, especially the gap junction (GJ) and fascia adherence (FA), observed between adjacent cells. Bile-like canaliculi (BLC) were occasionally observed between adjacent cells covered with MV. The differentiated HLCs contained large euchromatic nuclei (N), numerous mitochondria (M), developing Golgi apparatus (Go), rough and smooth endoplasmic reticuli (rES and sER), lysosome (Ly) and lipid droplets (L), and glycogen granules (G) in their cytoplasm.

3.2.2. Functional analysis

We assessed the activities of CYP2B1/2 and CYP1A1 according to

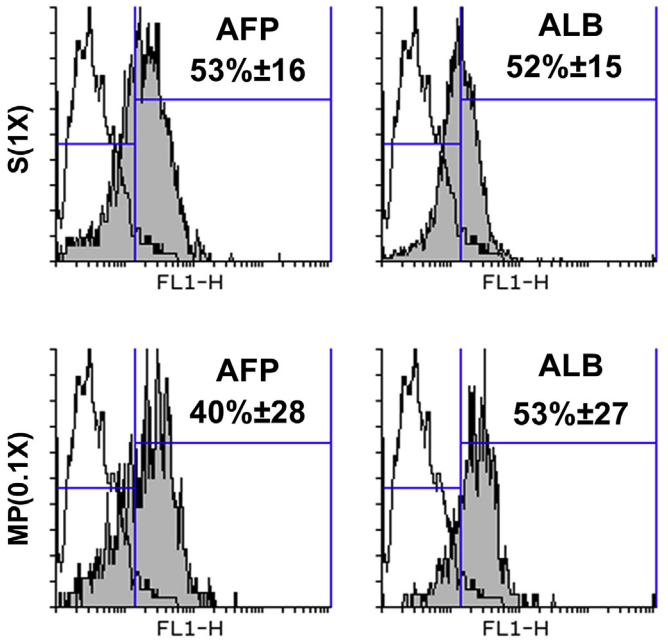

Fig. 5. Flow cytometry of hESC-HLCs. Flow cytometry analysis for α-fetoprotein (AFP) and albumin (ALB) was performed on dissociated and dispersed cells from spheroids on day 20. Cell spheroids treated with soluble GFs (upper row) and GF loaded MPs (lower row) groups had approximately the same amount of AFP- and ALB-positive cells.

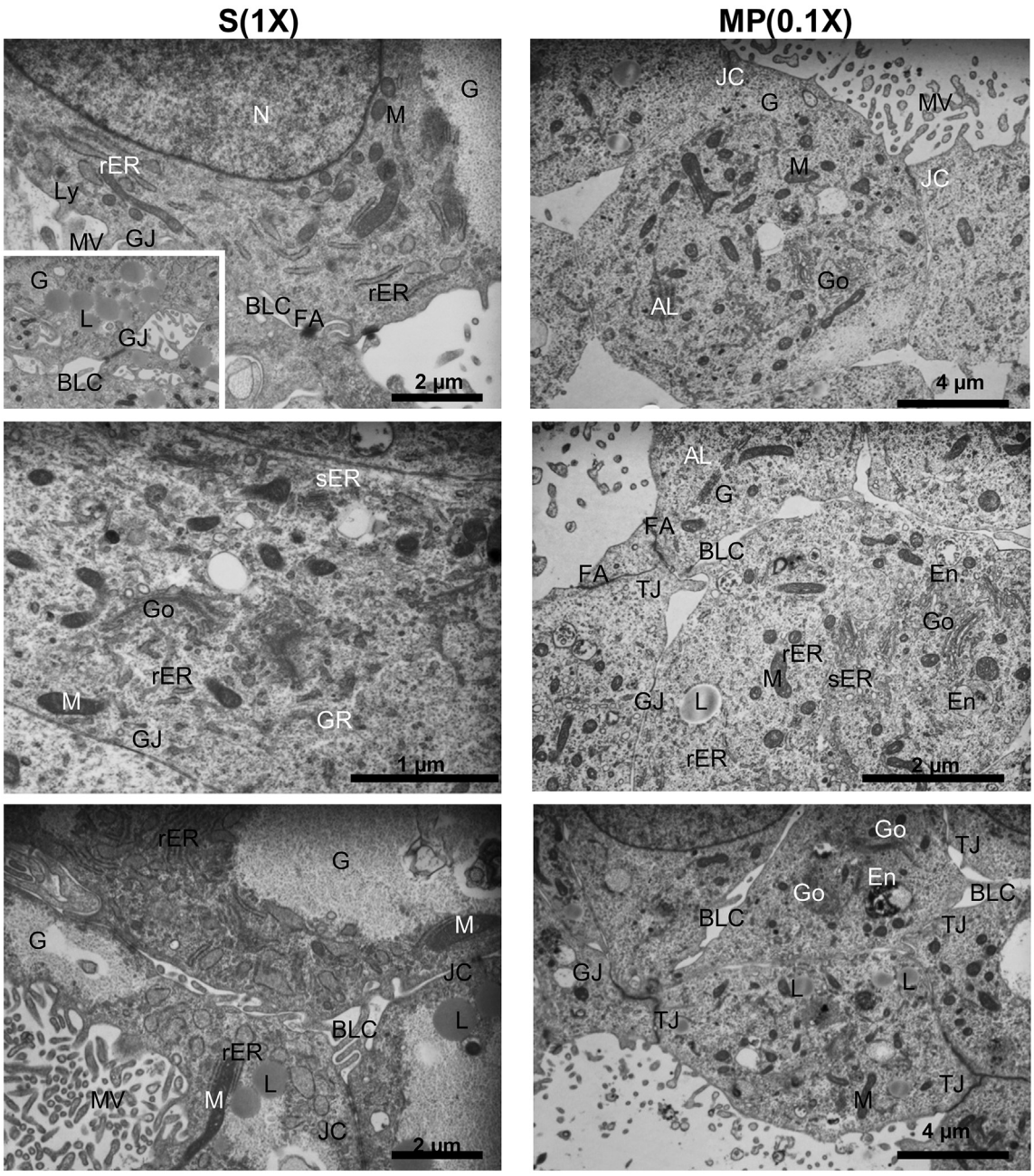

Fig. 6. Ultrastructural characteristics of hESC-HLCs. Transmission electron micrographs of HLCs in soluble (right panel) or MP (left panel) delivery of GFs to cell spheroids at day 20 indicate immature hepatocyte characteristics of the nucleus (N), mitochondria (M), Golgi apparatus (Go), lysosomes (Ly), lipid droplets (L), rough endoplasmic reticuli (rER), smooth endoplasmic reticuli (sER), glycogen granules (G), tight junction (TJ), gap junction (GJ), fascia adherence (FA), annulate lamellae (AL), junctional complex (JC), microvilli (MV), and bile-like canaliculus (BLC). There were no significant differences in ultrastructural characteristics observed between soluble- and MP-induced HLCs.

ethoxyresorufin-O-deethylase (EROD) and 7-pentoxyresorufin-O dealkylase (PROD) levels, respectively. In addition, the inducible hepatocytic CYP-mediated PROD and EROD activities were demonstrated before and after PB induction. We used fluorescence microscopy and related software to evaluate these results (Fig. 7A). In both groups, the fluorescence intensity of the supernatant medium increased significantly after 3 days of induction with PB; however, there were no significant differences in the S (1X) and MP (0.1X) groups (Fig. 7B).

HLCs in both groups showed uptake of ICG (Fig. 7C) and DiI-Ac-LDL (Fig. 7D). PAS staining showed glycogen storage in both groups (Fig. 7E). We assessed the cells for their ability to produce ALB and urea in culture. The results indicated that both groups produced similar levels of ALB (Fig. 7F) and urea (Fig. 7G). The ALB secretion and urea production of primary human hepatocytes were used as positive controls (Fig. 7F and G). As expected, the primary hepatocytes remarkably showed better physiologic function according to higher ALB secretion and urea production.

In order to assess whether the differentiated cells were engraftable, we transplanted 1×10^6 PKH-labeled HLCs into the spleens of cyclosporine-treated mice with acute liver damage after CCl4 treatment. After one week, we detected PKH-labeled HLCs in the livers of the transplanted animals by fluorescent microscopy. Most engrafted cells were detected near the pericentral zones.

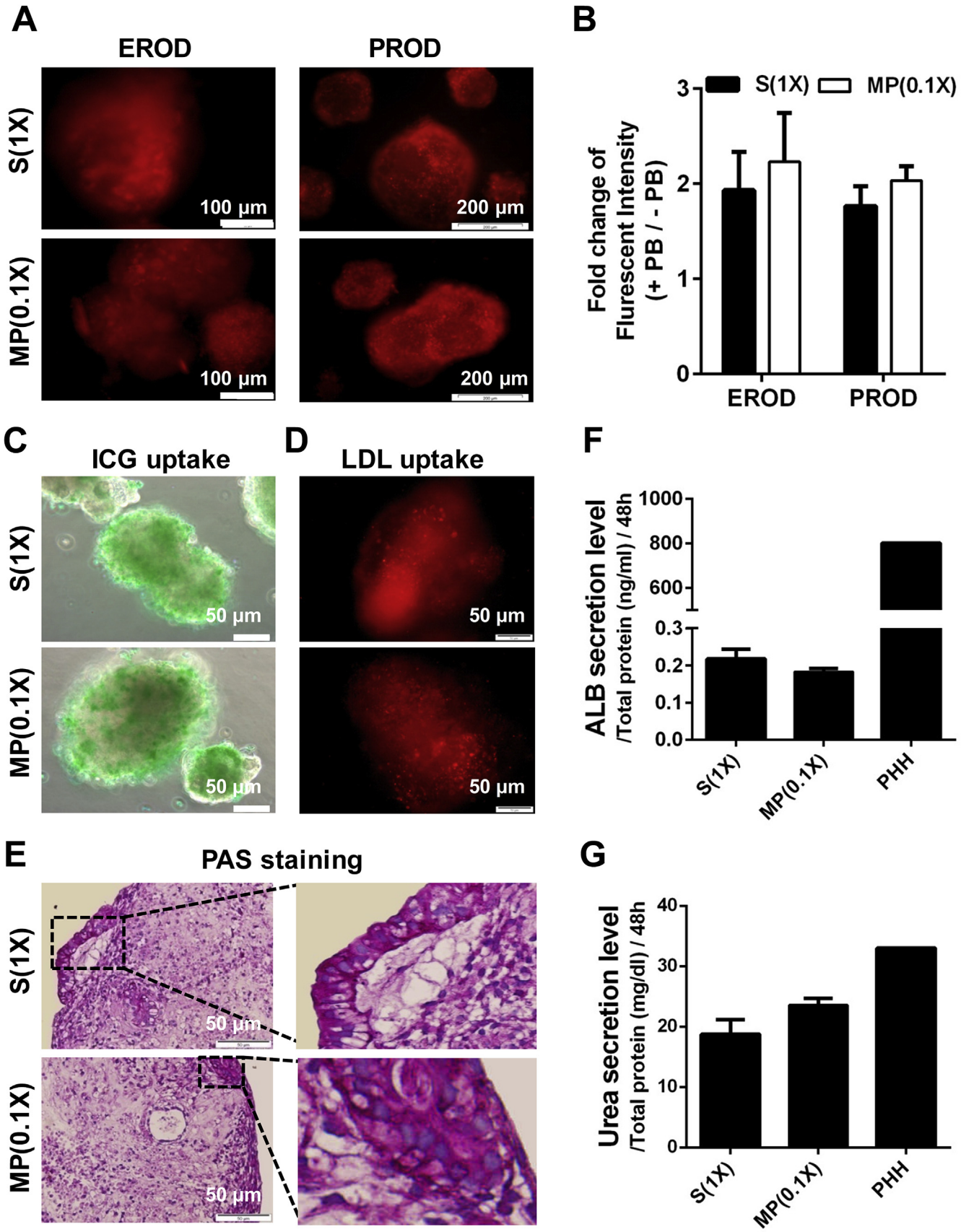

Fig. 7. Functional assay of hESC-HLCs. (A) CYP2B1/2 and CYP1A1 enzyme activities in the HLCs were evaluated by the pentoxyresorufin O-dealkylase (PROD) and ethoxyresorufin-O-deethylase (EROD) assays, respectively. (B) Fold change of fluorescence intensity in PROD and EROD assays analyzed before and after phenobarbital (PB) induction in HLC spheroid supernatant. (C) Microparticle (MP) and soluble HGF- and FGF4-treated HLC spheroids were examined for their ability to take up indocyanine green (ICG) and (D) DiI-Ac-LDL. (E) Periodic acid-Schiff (PAS) staining was performed on HLC spheroids with conventional soluble or MP-mediated delivery of GFs to analyze the levels of glycogen storage. (F) Albumin (ALB) secretion and (G) urea production were evaluated. No significant differences existed in each functional assay between the soluble and MP-based delivery of the GF. Human primary hepatocyte (PHH) was used as positive control for ALB secretion and urea production. All tests were performed in triplicate for each assay. $^{*}p < .05$ (student's t-test). Data are shown as mean ± SD ($n = 3$). (For interpretation of the references to color in this figure legend, the reader is referred to the Web version of this article.)

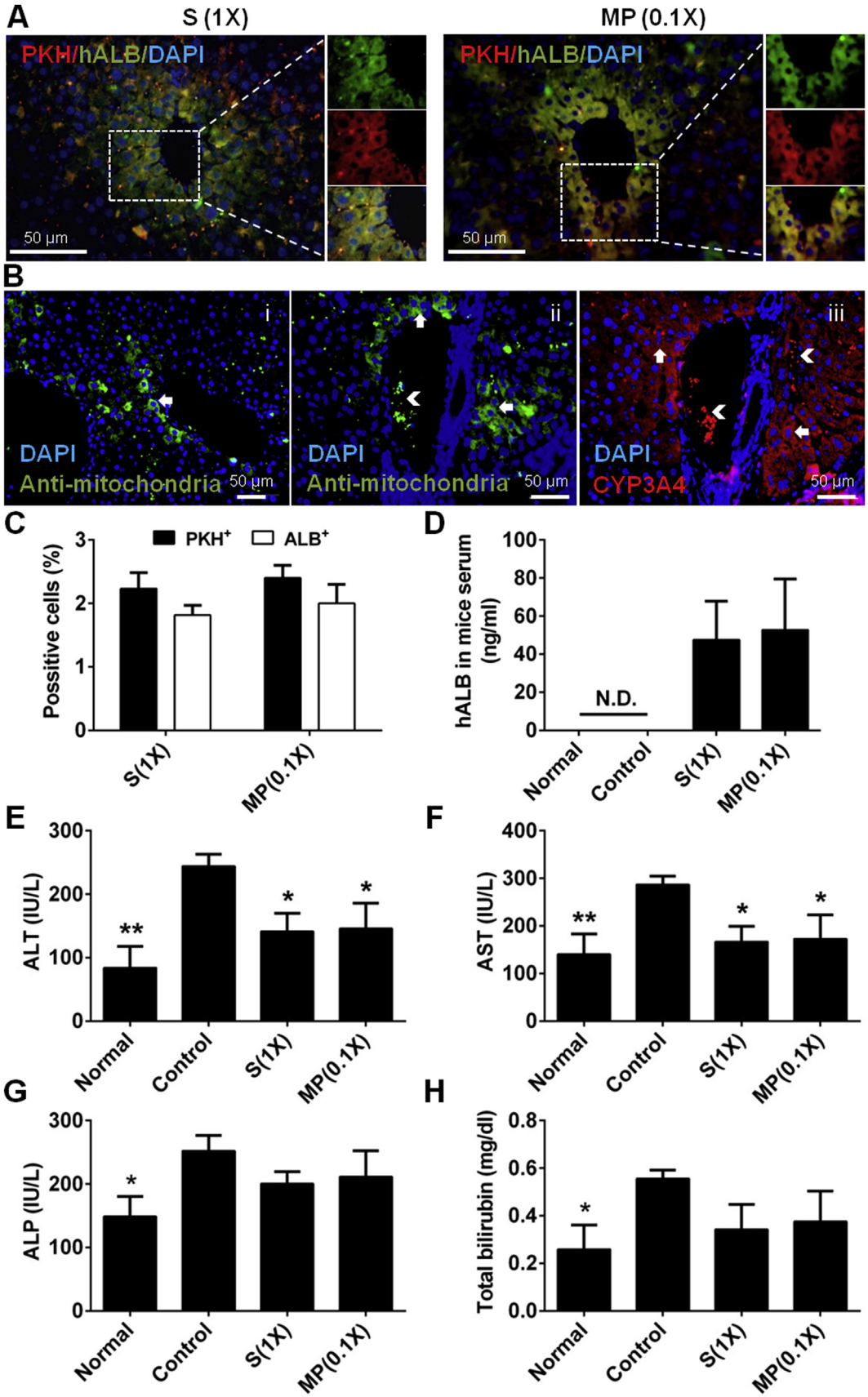

Fig. 8. Engraftment and functionality of HLCs in acute liver damaged mice. 1×10^6 PKH-labeled HLCs each from the soluble [S (1X)] or microparticle [MP (0.1X)] groups were transplanted into the spleens of carbon tetrachloride (CCl4)-treated immunosuppressed mice. The animals were evaluated 7 days after transplantation. (A) PKH-labeled cells (red) were detectable mostly around the central vein of the acute liver injury model in the S (1X) group and MP (0.1X) group as shown in the micrographs. The nuclei were counterstained

Double PKH/hALB positive cells were considered to be functionally transplanted HLCs (Fig. 8A). PKH-positive cells comprised approximately 2% within the recipient livers in both the soluble and MP groups (Fig. 8C). We noted that 80% of PKH positive cells were hALB positive in both groups. We also confirmed the presence of unlabeled human cells by immunofluorescence staining for human anti-mitochondria (Fig. 8B-i and ii) and the function by expression of CYP3A4 (Fig. 8B-iii). We measured hALB in the mice sera to explore the functionality of these PKH-positive transplanted cells. We detected 47.6 ± 20.3 ng/mL [S (1X) group] and 52.8 ± 26.8 ng/mL [MP (0.1X) group] hALB in the sera of these mice (Fig. 8D).

Finally, we measured changes in liver enzymes (ALT, AST, and ALP) and total bilirubin levels. The cell transplanted groups, S (1X) and MP (0.1X), were compared with the control (CCl4) group. There were significant decreases in the plasma levels of ALT (Fig. 8E) and AST (Fig. 8F) in animals treated with HLCs from both the S (1X) and MP (0.1X) groups compared with the control group. ALP plasma levels (Fig. 8G) and total bilirubin (Fig. 8H) decreased in the cell-transplanted groups. These decreases were not significant in both groups when compared to control group.

4. Discussion

A cost-effective, efficient protocol for scalable production of human desired cells such as hepatocytes from hPSCs is highly dependent on spatially and temporally controlled presentation of morphogenic factors. In this study, we have demonstrated that localized delivery of GFs by PLGA/PLLA MPs could be used as an efficient, cost-effective alternative to their soluble supplementation for scalable hepatocytic differentiation of hESCs in a 3D suspension culture. Compared to the conventional soluble delivery method, gene expression analyses showed that MP delivery of GFs resulted in similar expression levels of hepatocytic markers *ALB*, *AFP*, *CYP3A4*, *CYP3A7*, *HNF4α*, *E-cadherin*, *G6PC*, *TAT*, *TTR*, and *ASGPR* as well as at the protein level, despite the use of 10-fold less total GFs. Differentiated HLCs in the MP group showed ultrastructure and functional characteristics of glycogen storage, ICG uptake, ALB secretion, urea production, LDL uptake, and inducible cytochrome P450 activity comparable to the soluble GF group. HLCs in the MP group demonstrated successful engraftment into the liver and continued to present hepatocytic function as shown by ALB secretion after implantation and improvement in liver enzymes. These findings were comparable to the soluble GF group. In contrast, one-tenth of GFs in the soluble group, S (0.1X) or GF-free MPs, and MP (0) in spheroids did not lead to efficient hepatocytic differentiation.

These results agreed with other reports that demonstrated efficient differentiation of stem cell spheroids by MP delivery of various morphogens such as transforming growth factor-beta1 (TGF-β1) for chondrogenic differentiation of human MSC spheroids [20], nerve growth factor (NGF) for neural differentiation of mouse neural stem cell spheroids [22], bone morphogenic protein 4 (BMP4) to generate meiosis-competent germ cells from mouse ESCs [14], and retinoic acid to produce primitive streak cells from mouse ESC spheroids [16]. Qutachi et al. reported that MP delivery of multiple factors - simvastatin, BMP2, and VEGF within hESC aggregates facilitated localized osteogenic and vasculogenic differentiation [18]. Some studies reported that MP delivery within cell spheroids resulted in decreased consumption of GFs compared to the conventional soluble delivery method. For instance, MP delivery of BMP4 or noggin within mouse ESC spheroids induced efficient gene expression of mesoderm and ectoderm lineages, respectively despite the use of 12-fold fewer total GF [15]. Similarly, BMP4 and thrombopoietin delivery inside the mouse ESC spheroids resulted in efficient blood cell differentiation while GF consumption was reduced ~14.2-fold [17].

Interestingly, GF-loaded MPs resulted in less cystic spheroids at the final step of differentiation with mostly dense spheroids (Fig. 3A). In our previous study, we reported that cystic spheroids of hPSC-HLCs expressed mesoendodermal markers (*BRA*, *FAXA2*, *SOX17*) more than dense spheroids, whereas early and late hepatocytic markers (*HNF4a*, *AFP*, *ALB*, *TAT*, *CDH1*, *ASGPR1*) demonstrated higher upregulation in the dense spheroids [3].

The cells located in the marginal layers had better opportunity to exchange the necessary biomolecules with culture medium. The cells located in the core of the aggregates depended on simple diffusion to exchange crucial nutrients and biomolecules. This might be the reason for better demonstration of hepatocytic characteristics in the marginal layers.

As proof of concept, we demonstrated that HLCs generated from MP delivery of dual hepatogenic factors within hPSC spheroids transplanted intrasplenic into an acute liver injury model as single cells successfully engrafted within the liver tissue and continued to secret ALB. Notably, some reports suggested that localized and sustained delivery of HGF within cell encapsulated hydrogels would result in higher engraftment and maintenance of the HLCs *in vivo* [31,32]. However, transplantation of hepatocytes as multicellular spheroids is preferable for efficient engraftment and prolonged function *in vivo* [33]. Both requirements have been met in our developed GF-MP incorporated HLC spheroids. These composite spheroids can be considered as scaffold-free micro-tissues with endogenous sustained release of HGF, which can be transplanted as prepared and are highly expected to show great potential for *in vivo* engraftment and hepatocytic function. This approach is not possible by the use of recently developed FGF1 and HGF-releasing nanoparticles, which are solely applicable to single cells and require a scaffold for *in vivo* co-delivery of the cells and GFs [34]. Fabrication of MPs from biomaterials with engineered affinity to GFs, which are exogenously loaded in MPs or endogenously released from the cells during differentiation, may present an opportunity to sequester and harness signaling within 3D spheroids for more efficient differentiation [15]. Such an approach can target different GFs according to the differentiation method and desired cells.

In order to generate the MP-incorporated cell spheroids, we used the static liquid overlay where cultured dispersed hESCs in a non-adherent bacterial plate began to aggregate instead of adhering to the surface [35]. Until now, several fabrication methods have been used to create spheroids (for review see Ref. [36]) and include the hanging drop method [37], microwells [15,38], and spinner flasks to enable spontaneous cell aggregation [39,40]. More recently, cells have been seeded on non-adherent micropatterned surfaces in

with DAPI. Double PKH/ALB positive cells were detected as markers of functional activity of the transplanted HLCs. (B) We also confirmed the presence of unlabeled human cells by immunofluorescence staining for human anti-mitochondria (B-i and ii) and the function by expression of CYP3A4 (B-iii). The nuclei were counterstained with DAPI. The pictures ii and iii were took from two sequential sections. Arrows show positive cells and arrowheads indicate blood cells. (C) Quantification of HLC homing in the host liver. (D) Human ALB (hALB) was measured by ELISA in mice sera. (E–H) Biochemical assessment in blood sera of acute liver injury mice treated with hESC-HLCs. Cell transplantation led to significantly decreased alanine transaminase (ALT) and aspartate transaminase (AST) levels. Cell transplantation led to nonsignificant decreases in alkaline phosphatase (ALP) and total bilirubin levels. Data are shown as mean ± SD (n = 3). Statistical analysis as determined by one-way ANOVA with Tukey's post-hoc test *P < .05, **P < .01. Normal: Normal mice; Control: CCl4-treated mice; S (1X) and MP (0.1X): Cell-treated mice with GFs in S (1X) and MP (0.1X). (For interpretation of the references to color in this figure legend, the reader is referred to the Web version of this article.)

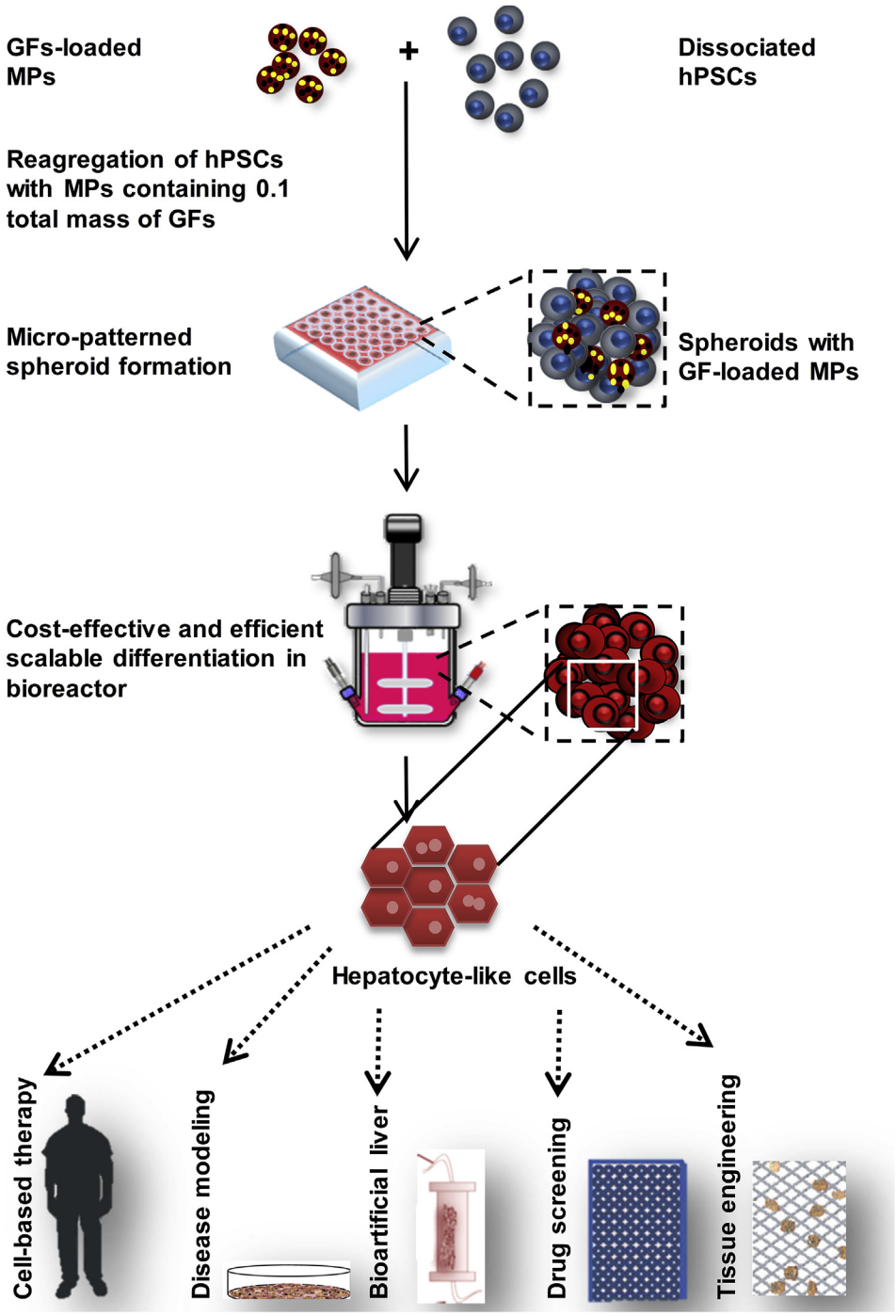

Fig. 9. Schematic presentation shows the manufacturing process for mass production of hPSC-HLCs by GF-releasing MPs in a stirred suspension bioreactor. The incorporation of GF-loaded biodegradable polymeric MPs within human pluripotent stem cell (hPSC) spheroids in 3D suspension culture resulted in efficient hepatocyte differentiation. To have a cost-benefit application of GFs in large-scale differentiation in bioreactor, the total concentration of GFs was reduced to one-tenth by using MPs. hPSCs aggregated with GF-loaded MPs through precipitation into multi wells of a micropatterned surface and generated high-throughput MP-incorporated 3D multicellular spheroids which subsequently provided large numbers of highly reproducible hepatocytic cells. This approach has provided a particularly attractive alternative for convectional supplementation of GFs for efficient and cost-effective scalable differentiation of suspension cultured hPSCs to HLCs. These HLCs have potential applications in drug discovery, disease model, bioartificial liver, tissue engineering, and regenerative medicine.

microfabricated devices [41]. These techniques provide 3D multicellular spheroids for high-throughput screening and the formation of complex, organotypic tissue grafts [42,43]. Therefore, the combination of high throughput methods with spheroid culture and GF-loaded MPs can lead to generation of highly reproducible hepatocytes in large numbers for biomedical applications (Fig. 9).

5. Conclusion

In this study, we demonstrated that the delivery of GFs by incorporation of biodegradable MPs within hESC spheroids resulted in a cost-effective, efficient hepatocytic differentiation compared to the conventional method. The importance of this

method pertains to the delivery and availability of GFs over a constant time. The cost for hepatocytic differentiation of one million initial hESCs using the proposed MP-delivery was reduced by 6.60-fold in comparison with the convectional (soluble) approach (Supplementary Tables S3 and S4). Frozen vials that included a total of 10×10^6 hPSCs could theoretically be thawed and, after 4 weeks, potentially produce up to 2×10^9 hPSCs in four spinner flasks that contain a total of 400 mL of medium [2]. By our MP delivery approach, a clinically relevant cell number of hPSC-HLCs (1×10^9 ALB-positive cells) theoretically could be produced in the same flasks over a 3-week period [3]. Our approach prompted investigation of pairing small molecules and GFs, along with material interactions for more sophisticated spatiotemporal controlled delivery of GFs within hPSC spheroids. This approach could provide wide applications in drug discovery, bio-artificial liver devices, tissue engineering, and regenerative medicine.

Conflicts of interest

The authors declare that they do not have any conflicts of interest.

Author contributions

Z.H., M.G. and H.B. conceived this study. Z.H. performed and analyzed biological experiments and wrote the first draft of the manuscript. M.G and M.A. performed and analyzed engineering experiments and wrote the engineering part of the manuscript. Z.F. optimized the hepatocytic protocol differentiation. M.R.L. prepared hESC spheroid cultures. M.N. performed the immunofluorescence staining in the transplanted liver. A.P. performed the ultrastructure analysis. M.V. analyzed experiments and discussed the results. H.B. provided financial support, designed and analyzed the experiments, discussed the results, wrote the paper, and approved the manuscript. All authors approved the final manuscript.

Acknowledgement

This study was funded by grants from Royan Institute, the Iranian Council of Stem Cell Research and Technology, the Iran National Science Foundation, and Iran Science Elites Federation. We would like to express our gratitude to Dr. Mohammad Hassan Asghari-Vostikolaee for his assistance in performing the animal studies, in addition to Mehdi Alikhani, and Dr. Behshad Pournasr for their critical comments and technical supports. We express our appreciation to all members of the Hepatocyte Program at Royan Institute for their helpful deliberation and consultation during this work. All authors approved the final manuscript.

Appendix A. Supplementary data

Supplementary data related to this article can be found at https://doi.org/10.1016/j.biomaterials.2018.01.005.

References

[1] S.N. Bhatia, G.H. Underhill, K.S. Zaret, I.J. Fox, Cell and tissue engineering for liver disease, Sci. Transl. Med. 6 (2014), 245sr2.
[2] S. Abbasalizadeh, M.R. Larijani, A. Samadian, H. Baharvand, Bioprocess development for mass production of size-controlled human pluripotent stem cell aggregates in stirred suspension bioreactor, Tissue Eng. C Meth. 18 (2012) 831–851.
[3] M. Vosough, E. Omidinia, M. Kadivar, M.A. Shokrgozar, B. Pournasr, N. Aghdami, et al., Generation of functional hepatocyte-like cells from human pluripotent stem cells in a scalable suspension culture, Stem Cell. Dev. 22 (2013) 2693–2705.
[4] K. Takayama, K. Kawabata, Y. Nagamoto, K. Kishimoto, K. Tashiro, F. Sakurai, et al., 3D spheroid culture of hESC/hiPSC-derived hepatocyte-like cells for drug toxicity testing, Biomaterials 34 (2013) 1781–1789.
[5] T. Imamura, L. Cui, R. Teng, K. Johkura, Y. Okouchi, K. Asanuma, et al., Embryonic stem cell-derived embryoid bodies in three-dimensional culture system form hepatocyte-like cells in vitro and in vivo, Tissue Eng. 10 (2004) 1716–1724.
[6] S. Wang, D. Nagrath, P.C. Chen, F. Berthiaume, M.L. Yarmush, Three-dimensional primary hepatocyte culture in synthetic self-assembling peptide hydrogel, Tissue Eng. 14 (2008) 227–236.
[7] A. Skardal, L. Smith, S. Bharadwaj, A. Atala, S. Soker, Y. Zhang, Tissue specific synthetic ECM hydrogels for 3-D in vitro maintenance of hepatocyte function, Biomaterials 33 (2012) 4565–4575.
[8] M.W. Laschke, M.D. Menger, Life is 3D: boosting spheroid function for tissue engineering, Trends Biotechnol. 35 (2017) 133–144.
[9] E. Sachlos, D.T. Auguste, Embryoid body morphology influences diffusive transport of inductive biochemicals: a strategy for stem cell differentiation, Biomaterials 29 (2008) 4471–4480.
[10] A.P. Van Winkle, I.D. Gates, M.S. Kallos, Mass transfer limitations in embryoid bodies during human embryonic stem cell differentiation, Cells Tissues Organs 196 (2012) 34–47.
[11] A.M. Bratt-Leal, R.L. Carpenedo, T.C. McDevitt, Engineering the embryoid body microenvironment to direct embryonic stem cell differentiation, Biotechnol. Prog. 25 (2009) 43–51.
[12] M.A. Kinney, T.C. McDevitt, Emerging strategies for spatiotemporal control of stem cell fate and morphogenesis, Trends Biotechnol. 31 (2013) 78–84.
[13] M.A. Kinney, T.A. Hookway, Y. Wang, T.C. McDevitt, Engineering three-dimensional stem cell morphogenesis for the development of tissue models and scalable regenerative therapeutics, Ann. Biomed. Eng. 42 (2014) 352–367.
[14] F. Esfandiari, M.K. Ashtiani, M. Sharifi-Tabar, M. Saber, H. Daemi, M.H. Ghanian, et al., Microparticle-mediated delivery of BMP4 for generation of meiosis-competent germ cells from embryonic stem cells, Macromol. Biosci. (2017) 17.
[15] A.M. Bratt-Leal, A.H. Nguyen, K.A. Hammersmith, A. Singh, T.C. McDevitt, A microparticle approach to morphogen delivery within pluripotent stem cell aggregates, Biomaterials 34 (2013) 7227–7235.
[16] R.L. Carpenedo, A.M. Bratt-Leal, R.A. Marklein, S.A. Seaman, N.J. Bowen, J.F. McDonald, et al., Homogeneous and organized differentiation within embryoid bodies induced by microsphere-mediated delivery of small molecules, Biomaterials 30 (2009) 2507–2515.
[17] K.A. Purpura, A.M. Bratt-Leal, K.A. Hammersmith, T.C. McDevitt, P.W. Zandstra, Systematic engineering of 3D pluripotent stem cell niches to guide blood development, Biomaterials 33 (2012) 1271–1280.
[18] O. Qutachi, K.M. Shakesheff, L.D. Buttery, Delivery of definable number of drug or growth factor loaded poly(DL-lactic acid-co-glycolic acid) microparticles within human embryonic stem cell derived aggregates, J. Contr. Release 168 (2013) 18–27. Official Journal of the Controlled Release Society.
[19] G. Della Porta, B.N. Nguyen, R. Campardelli, E. Reverchon, J.P. Fisher, Synergistic effect of sustained release of growth factors and dynamic culture on osteoblastic differentiation of mesenchymal stem cells, J. Biomed. Mater. Res. 103 (2015) 2161–2171.
[20] L.D. Solorio, A.S. Fu, R. Hernandez-Irizarry, E. Alsberg, Chondrogenic differentiation of human mesenchymal stem cell aggregates *via* controlled release of TGF-beta1 from incorporated polymer microspheres, J. Biomed. Mater. Res. 92 (2010) 1139–1144.
[21] M. Govoni, A.C. Berardi, C. Muscari, R. Campardelli, F. Bonafe, C. Guarnieri, et al., An engineered multiphase three-dimensional microenvironment to ensure the controlled delivery of cyclic strain and human growth differentiation factor 5 for the tenogenic commitment of human bone marrow mesenchymal stem cells, Tissue Eng. Part A 23 (15–16) (2017) 811–822.
[22] M.J. Mahoney, W.M. Saltzman, Transplantation of brain cells assembled around a programmable synthetic microenvironment, Nat. Biotechnol. 19 (2001) 934–939.
[23] H. Baharvand, S.K. Ashtiani, A. Taee, M. Massumi, M.R. Valojerdi, P.E. Yazdi, et al., Generation of new human embryonic stem cell lines with diploid and triploid karyotypes, Dev. Growth Differ. 48 (2006) 117–128.
[24] H. Baharvand, M.R. Larijani, M. Yousefi, Protocol for expansion of undifferentiated human embryonic and pluripotent stem cells in suspension, Methods Mol. Biol. 873 (2012) 217–226.
[25] J.O. Hollinger, K. Leong, Poly(alpha-hydroxy acids): carriers for bone morphogenetic proteins, Biomaterials 17 (1996) 187–194.
[26] M.S. Shive, J.M. Anderson, Biodegradation and biocompatibility of PLA and PLGA microspheres, Adv. Drug Deliv. Rev. 28 (1997) 5–24.
[27] A.M. Bratt-Leal, R.L. Carpenedo, M.D. Ungrin, P.W. Zandstra, T.C. McDevitt, Incorporation of biomaterials in multicellular aggregates modulates pluripotent stem cell differentiation, Biomaterials 32 (2011) 48–56.
[28] M. Totonchi, A. Taei, A. Seifinejad, M. Tabebordbar, H. Rassouli, A. Farrokhi, et al., Feeder- and serum-free establishment and expansion of human induced pluripotent stem cells, Int. J. Dev. Biol. 54 (2010) 877–886.
[29] H. Baharvand, S.M. Hashemi, M. Shahsavani, Differentiation of human embryonic stem cells into functional hepatocyte-like cells in a serum-free adherent culture condition, Differentiation 76 (2008) 465–477. Research in Biological Diversity.
[30] H. Baharvand, S.M. Hashemi, S. Kazemi Ashtiani, A. Farrokhi, Differentiation of human embryonic stem cells into hepatocytes in 2D and 3D culture systems in vitro, Int. J. Dev. Biol. 50 (2006) 645–652.

[31] S. Pulavendran, M. Rajam, C. Rose, A.B. Mandal, Hepatocyte growth factor incorporated chitosan nanoparticles differentiate murine bone marrow mesenchymal stem cell into hepatocytes in vitro, IET Nanobiotechnol. 4 (2010) 51–60.
[32] C.H. Chiang, W.W. Wu, H.Y. Li, Y. Chien, C.C. Sun, C.H. Peng, et al., Enhanced antioxidant capacity of dental pulp-derived iPSC-differentiated hepatocytes and liver regeneration by injectable HGF-releasing hydrogel in fulminant hepatic failure, Cell Transplant. 24 (2015) 541–559.
[33] D.S. Ham, M.S. Song, H.S. Park, M. Rhee, H.K. Yang, S.H. Lee, et al., Successful xenotransplantation with re-aggregated and encapsulated neonatal pig liver cells for treatment of mice with acute liver failure, Xenotransplantation 22 (2015) 249–259.
[34] M. Wang, X. Yang, P. Zhang, L. Cai, X. Yang, Y. Chen, et al., Sustained delivery growth factors with polyethyleneimine-modified nanoparticles promote embryonic stem cells differentiation and liver regeneration, Adv. Syst. 3 (2016), 1500393.
[35] J.M. Yuhas, A.P. Li, A.O. Martinez, A.J. Ladman, A simplified method for production and growth of multicellular tumor spheroids, Canc. Res. 37 (1977) 3639–3643.
[36] E. Fennema, N. Rivron, J. Rouwkema, C. van Blitterswijk, J. de Boer, Spheroid culture as a tool for creating 3D complex tissues, Trends Biotechnol. 31 (2013) 108–115.
[37] H. Kurosawa, Methods for inducing embryoid body formation: in vitro differentiation system of embryonic stem cells, J. Biosci. Bioeng. 103 (2007) 389–398.
[38] G. Pettinato, X. Wen, N. Zhang, Formation of well-defined embryoid bodies from dissociated human induced pluripotent stem cells using microfabricated cell-repellent microwell arrays, Sci. Rep. 4 (2014) 7402.
[39] M.R. Larijani, A. Seifinejad, B. Pournasr, V. Hajihoseini, S.N. Hassani, M. Totonchi, et al., Long-term maintenance of undifferentiated human embryonic and induced pluripotent stem cells in suspension, Stem Cell. Dev. 20 (2011) 1911–1923.
[40] R.L. Carpenedo, C.Y. Sargent, T.C. McDevitt, Rotary suspension culture enhances the efficiency, yield, and homogeneity of embryoid body differentiation, Stem Cell. 25 (2007) 2224–2234.
[41] N.C. Rivron, J. Rouwkema, R. Truckenmuller, M. Karperien, J. De Boer, C.A. Van Blitterswijk, Tissue assembly and organization: developmental mechanisms in microfabricated tissues, Biomaterials 30 (2009) 4851–4858.
[42] L.S. Moreira Teixeira, J.C. Leijten, J. Sobral, R. Jin, A.A. van Apeldoorn, J. Feijen, et al., High throughput generated micro-aggregates of chondrocytes stimulate cartilage formation in vitro and in vivo, Eur. Cell. Mater. 23 (2012) 387–399.
[43] E. Gevaert, L. Dolle, T. Billiet, P. Dubruel, L. van Grunsven, A. van Apeldoorn, et al., High throughput micro-well generation of hepatocyte micro-aggregates for tissue engineering, PLos One 9 (2014), e105171.